

# POWER QUALITY IMPROVEMENT OF ELECTRICAL SUB-NETWORKS WITH MULTIFUNCTIONAL PV-INVERTERS FOR INDUSTRIAL CUSTOMERS

D. Geibel

Institut fuer Solare Energieversorgungstechnik e. V. (ISET), Koenigstor 59, D-34119 Kassel, Germany  
Phone +49(0)561/7294-211, Fax +49(0)561/7294-400, E-mail: dgeibel@iset.uni-kassel.de

**ABSTRACT:** This paper introduces a Multifunctional PV-Inverter and its application for Power Quality improvement in electrical sub-networks. Measurement results point out the potential of this Multifunctional PV-Inverter concerning protection of sensitive loads against voltage variations, voltage dips and harmonics beside the conventional injection of PV-energy.

**Keywords:** Multifunctional Photovoltaic Inverter, Large Grid-connected PV systems, Industrial Application, Power Quality

## 1 INTRODUCTION

PV-systems offer large potentials including additional functionality. Within a research project funded by the German government a PV-Inverter in the range of 100 kVA is being developed that additionally is able to provide uninterruptable power supply functionality, local Power Quality (PQ) improvement as well as ancillary services such as peak shaving by using a battery storage. Such systems are of economical interest since the combination of two systems is less expensive [1] and PV energy is priced at special tariffs in several European countries.

This paper focuses on possibilities improving Power Quality (PQ) for industrial customers by using a Multifunctional PV-Inverter (Multi-PV). Therefore the behaviour on voltage variations and harmonics is going to be assessed by measurements using a laboratory sample of the described Multi-PV System.

## 2 MULTIFUNCTIONAL PV-INVERTER SYSTEMS

Figure 1 presents a schematic of the Multi-PV and the integration into industrial grids. The industrial grid with the Multi-PV can be treated as an Active Customer Network connected to the public Distribution Network (ACN-DN) [2].

Based on state of the art grid connected PV-Inverters, additional battery storage, decoupling inductor and fast circuit breaker are required. The battery storage is coupled through a DC/DC converter to the DC-link in order to allow an optimal usage of PV-energy.

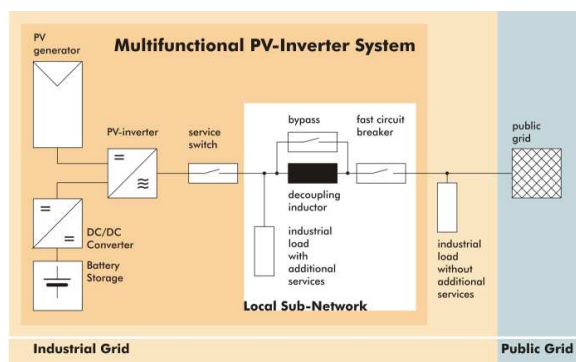


**Figure 1:** Schematic of the Multi-PV and system integration into industrial grids

The AC output of the inverter in combination with decoupling inductor forms a sub-network in which voltage can be controlled almost independently from voltage in the superior grid [3], [4]. This control is achieved by injection of reactive power providing constant and lowly distorted voltage to dedicated loads of the sub-network.

Three switches control the load flow. For isolating the local sub-network in case of a grid fault of the superior grid the fast circuit breaker is used. In order to minimise losses and to test features that can not be combined with decoupled operation the inductor can be bypassed. During maintenance the inverter can be separated by a service switch while the dedicated loads are supplied by the superior grid. [5]

### 2.1 Additional functionality

Beside named hardware changes mainly software adjustments of control algorithms and operating methods have to be adapted for applying additional functionalities. A brief overview is given below. [5]

- **Feed-in of PV energy:**  
Special tariff for PV energy demands the optimal feed-in at the highest possible efficiency.
- **Local PQ Improvement:**  
Using the decoupling inductor the voltage profile can be locally improved. Sensitive loads in the local sub-network will be protected from being affected by voltage variations and disturbances. Since the voltage control is achieved by injection of reactive power, the exchange with the superior grid can not be fully controlled anymore.
- **UPS**  
Sensitive loads will be protected from outages in terms of both high and low impedance faults of the superior grid by switching the fast circuit breaker. In this case sensitive loads will be supplied with battery energy; PV will extend maximum duration of supply.
- **Peak Shaving**  
Energy cost for industrial customers depend inter alia on the peak power demand. Reducing the peak power by injecting energy from the battery storage can reduce total energy costs.

- **Supply of Control Energy**  
Principally this functionality is similar to the previously mentioned peak shaving capability. The only difference is the accounting grid. While peak shaving will be used for special contract customers control energy is tendered in special portions.

- **Reactive Power Compensation**  
It is useful to minimise reactive power demand by local compensation, because industrial customers have to pay for their reactive power demand. Set values can either be served externally or internally in order to compensate the reactive power demand of dedicated loads. Therefore the serial inductor has to be bypassed.

- **Harmonics Compensation**  
Supplying lower order harmonics (e.g. 5<sup>th</sup>, 7<sup>th</sup> or 11<sup>th</sup>) in a controlled way by the inverter can compensate these. Set values can be served similar to reactive power supply/compensation. For this function the serial inductor has to be bypassed, too.

## 2.2 Options and restrictions for combined functionality

Taking into account the principle of decoupled sub-networks used for local voltage control and UPS functionality, it is not possible to combine all described functionality together. Table I presents an overview of possible combinations of the different functionalities.

**Table I:** Possible functionality depending on the system configuration, modified from [5]

Function	With Decoupling Inductor	Without Decoupling Inductor
Feed-in of PV energy	yes	yes
Local PQ Improvement	yes	no
UPS Functionality	yes	yes/no <sup>1</sup>
Provision of Control Energy	yes	yes
Peak Shaving	yes	yes
Reactive Power Supply/Compensation at PCC <sup>2</sup>	no	yes
Harmonics Compensation at PCC <sup>2</sup>	no	yes

## 2.3 Laboratory sample of the Multi-PV

A laboratory sample of the Multi-PV System has been built in cooperation with SMA Solar Technology AG (SMA). Basic electrical specifications are given in Table II. The PV-Inverter with additional decoupling inductor, fast circuit breaker and DC/DC-converter is shown in Figure 2. The battery storage container is presented in Figure 3.

**Table II:** Electrical specification of the Multi-PV laboratory sample

nominal power	100 kVA
decoupling inductor	configurable 0.3 mH - 1.8 mH

<sup>1</sup> Depending on the UPS classification according to EN 62040-3

<sup>2</sup> PCC: Point of common coupling

battery storage	384 V, 800 Ah
PV Generator	100 kW <sub>p</sub> PV simulator



**Figure 2:** Laboratory sample of the Multi-PV at ISET's testing centre DeMoTec



**Figure 3:** Battery storage with system voltage of 384 V consisting of 192 single cells.

## 3 CONTROL METHODS FOR MULTI-FUNCTIONAL PV-INVERTER SYSTEMS

Due to the additional decoupling inductor of the Multi-PV the network line parameters will change. Therefore control methods have to consider this behaviour. Before showing these in detail some theoretical notes about energy transmission in networks are given.

### 3.1 Energy transmission in networks

Regarding distribution and transmission networks the mechanism of energy transmission differs because of unequal line parameters. Distribution networks, basically at the low voltage level, are dominated by a ohmic resistance load per unit length. In contrast transmission networks, principally at the high voltage level, have an inductive character. The ratio between resistive and inductive character of networks can be specified with the R/X value.  $R/X > 1$  indicates a resistive behaviour, while  $R/X < 1$  suggests an inductive one. Table III shows typical parameters of electrical lines for different voltage levels and the corresponding R/X-ratio.

**Table III:** Typical parameters of electrical lines [6]

Voltage level	R [ $\Omega$ /km]	X [ $\Omega$ /km]	R/X
Low voltage	0.642	0.083	7.7
Medium voltage	0.161	0.190	0.85
High voltage	0.06	0.191	0.31

For assessing active and reactive power flow mechanisms in networks for different line parameters, an equivalent circuit diagram consisting of two voltage

sources ( $V_1, V_2$ ) coupled by a network line with parameters for the resistive and the inductive part (cp. Figure 4 left) is used. The pointer diagram on the right side of Figure 4 describes the relation between the two voltage sources by the RMS value and the phase difference angle  $\delta$  between them.

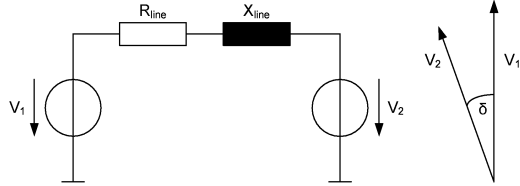


**Figure 4:** Coupling of two voltage source with resistive and inductive line parameters on the left, pointer diagram on the right. [4]

Results of general calculations for active power flow  $P$  and reactive power flow  $Q$  are given in following two equations below.  $P$  and  $Q$  are depending from  $R_{line}$ ,  $X_{line}$ ,  $V_{1,rms}$ ,  $V_{2,rms}$  and the phase angle  $\delta$  (cp. Figure 4).

$$P = \left( \frac{R_{line} \cdot (V_{1,rms}^2 - V_{1,rms} \cdot V_{2,rms} \cdot \cos(\delta)) + X_{line} \cdot V_{1,rms} \cdot V_{2,rms} \cdot \sin(\delta)}{R_{line}^2 + X_{line}^2} \right)$$

$$Q = \left( \frac{X_{line} \cdot (V_{1,rms}^2 - V_{1,rms} \cdot V_{2,rms} \cdot \cos(\delta)) + R_{line} \cdot V_{1,rms} \cdot V_{2,rms} \cdot \sin(\delta)}{R_{line}^2 + X_{line}^2} \right)$$

In case of resistive coupled networks, the parameter  $X_{line}$  could be neglected, for inductive coupled networks the parameter  $R_{line}$ . Simplifying the equations result in Table IV which describes the mechanism for active and reactive power flow in networks.

**Table IV:** Energy transmission mechanism in resistive and inductive networks

	Resistive coupled networks	Inductive coupled networks
Active Power Flow	Voltage difference	Phase difference
Reactive Power Flow	Phase difference	Voltage difference

### 3.2 Control for functions using the decoupling inductor

By using the decoupling inductor the predominantly resistive character of low voltage lines is shifted to an inductive one ( $R/X > 1$ ). As shown in Table IV changes of mechanism for active and reactive power flow are considered in the control algorithm pictured in Figure 5.

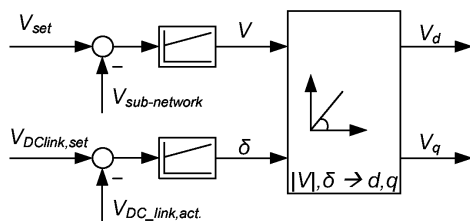


**Figure 5:** Control algorithm for inductive decoupled networks

The voltage amplitudes of the sub-network voltages are kept at a constant set point using a PI-controller. Within certain limits the voltage amplitudes of the sub-network can be controlled independently from the grid voltages, differences between voltages amplitudes from sub-network and grid result in a reactive power flow.

Active power flow is realised by making a phase difference between the voltages of the sub-network and the grid. This phase difference is controlled by a PI-controller with the input values of the DC-link voltage. The set point for the DC-link voltage is given by the MPP-controller for an optimal feed-in of PV-energy.

### 3.3 Control for functions not using the decoupling inductor

Bypassing the decoupling inductor the control for active power flow can be similar to state of the art PV-inverters (cp. Figure 6). Feed-in of PV-energy is controlled by the d-component using a PI-controller for the DC-link voltage.

Regarding the reactive power flow, standard PV-inverters have a set point for the q-component equal to zero. For using the Multi-PV e.g. for reactive power compensation or supply this set point has to be adjusted according to the requirements.

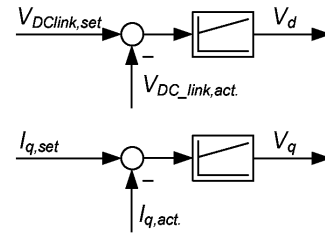


**Figure 6:** Control algorithm for resistive coupled networks

## 4 POWER QUALITY IMPROVEMENT WITH THE MULTI-PV SYSTEM

This section describes the possibilities of the Multi-PV System to improve local PQ for sensitive loads in the sub-network. Three types of voltage disturbances are assessed; firstly steady-state voltage variations, secondly transient voltage variations and thirdly voltage waveform distortion by means of harmonic content.

### 4.1 Steady-state voltage variations

Voltage tolerance bands are described in several norms. According to EN 61000-2-4 class 2 for industrial grids the voltage level should stay within limits of  $230 V_{RMS} \pm 10\%$ .

The Multi-PV provides the opportunity to compensate voltage deviations for sensitive loads operating within an industrial grid if they are connected to the local sub-network. This behaviour can be achieved by using the control scheme shown in Figure 5. Direct control of the sub-network voltage is feasible.

For testing purposes, the grid voltages are varied slowly within  $230 V_{RMS} \pm 10\%$ . In Figure 7 measurements of the grid voltage and sub-network voltage of phase 1 during these steady state voltage variations are presented. The sub-network voltages stay

constant at the set point of 230 V during the grid voltages variations.

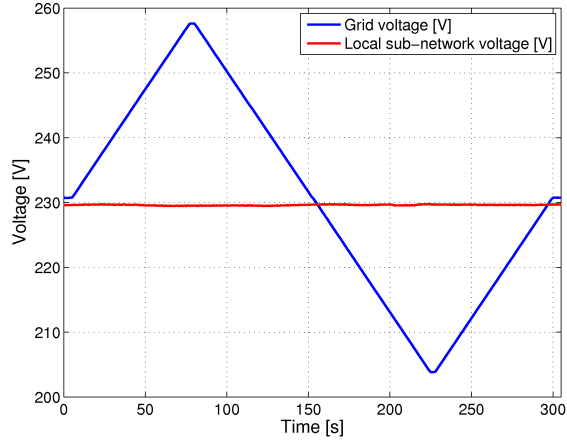


**Figure 7:** Measured sub-network voltage during an applied grid voltage ramp of  $230 \text{ V}_{\text{RMS}} \pm 10 \%$

For controlling the sub-network voltages to a constant value additional injection of reactive power is required. The amount depends on several parameters. Following equation points out the dependencies where  $P_{MPV}$  is the injected active power of the inverter (PV-energy and/or energy from the battery),  $S_{sub-net}$  the apparent power and  $\cos(\varphi_{sub-net})$  the power factor of loads in the local sub-network,  $L_{Dec}$  the value of the decoupling inductor and  $V_{Grid}$  the grid voltage:

$$Q_{Inv} = f(P_{MPV}, S_{sub-net}, \cos(\varphi_{sub-net}), L_{Dec}, V_{Grid})$$

Evaluating the influence of these parameters several measurements are performed by varying selected parameters. In Figure 8 results for the three phase reactive power for different values of the decoupling inductor and constant load and injection conditions are shown.

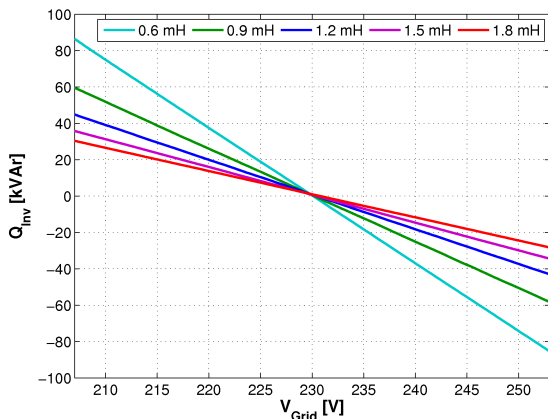


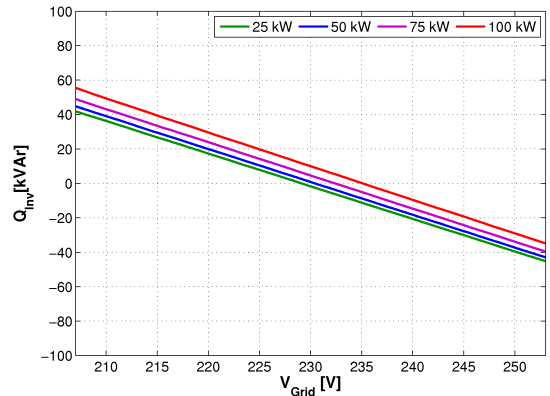
**Figure 8:** Measured three phase reactive power of the inverter. For  $Q > 0$  injection of capacitive reactive power. Parameters:  $P_{MPV} = 25 \text{ kW}$ ,  $P_{sub-net} = 50 \text{ kW}$ ,  $L_{Dec} = 0.6 \text{ mH} \dots 1.8 \text{ mH}$ .

The reactive power demand rises for smaller values of the decoupling inductor and comparable grid voltages. Especially for values smaller than 1.2 mH a high increase of injected reactive power amount is detected.

As mentioned the additional reactive power also depends on sub-network load conditions and active power injection of the Multi-PV. These two parameters distinguish the active power  $P_{Dec}$  which flows through the decoupling inductor between sub-network and grid.

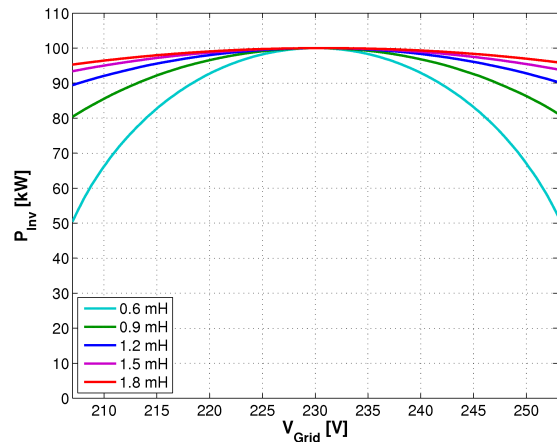
$$P_{Dec} = P_{MPV} - S_{sub-net} \cdot \cos(\varphi_{sub-net})$$

Figure 9 shows the reactive power amount for different sub-network load conditions and constant active power injection of the Multi-PV. A decoupling inductor with 1.2 mH is used. For higher active power flow between the grid and the local sub-network, a constant amount of reactive power is added compared to an operation with no active power exchange.



**Figure 9:** Measured three phase reactive power for  $P_{MPV} = 25 \text{ kW}$ ,  $L_{Dec} = 1.2 \text{ mH}$  and different sub-network load conditions. For  $Q > 0$  injection of capacitive reactive power.

Assuming the nominal apparent power of the Multi-PV the additional reactive power injection for compensating steady state grid voltage variations reduces the maximal possible active power injection. Figure 10 shows the maximal possible active power injection at varying grid voltages. It has to be mentioned that changes of reactive power for different active power injections of the PV-inverter and load conditions in the sub-network are neglected for simplification.



**Figure 10:** Calculated maximal active power injection on the basis of measurement results for several values of the decoupling inductor

The measurement results confirm that steady state voltage variations can be compensated for sensitive loads connected to the local sub-network. The additional needed reactive power mainly depends on the decoupling inductor for comparable grid deviations. Smaller values of the decoupling inductor cause higher amounts of reactive power but lower ohmic losses. Therefore the possible active power injection of the PV-Inverter decreases if voltage variations occur. For choosing the value of the decoupling inductor the above mentioned points has to be considered.

#### 4.2 Transient voltage variations

The effect of transient voltage variations for sensitive loads can be damped by using the decoupling inductor. For voltage dips with low depths, the remaining voltage is over 80 % of the nominal grid voltage, the control of the Multi-PV injects reactive current. If the voltage dip is below 80 % of the nominal grid voltage the up-functionality secures the loads in the sub-network. Here, only voltage dips with more than 80 % of remaining voltage are regarded.

For evaluation voltage dips with a remaining voltage of 85% of the nominal voltage are analysed. Therefore several duration times (70 ms, 100 ms) and phase angles ( $0^\circ$ ,  $90^\circ$ ) are considered. Because the Multi-PV is a three phase system the phase angles are related to phase 1. Voltage dips for one, two and three phases variations are performed.

Transient voltages and currents of phase 1 during a voltage dip are shown in Figure 11. The grid voltage and the load voltage in the sub-network can be seen in the upper picture, the inverter and load current in the lower. The voltage dip lasts 100 ms and the starting phase angle is  $90^\circ$ . The sub-network load consumes 100 kW while the Multi-PV-inverter is injecting 50 kW.

In evidence the sub-network load voltage can not be hold at the set point of  $230 \text{ V}_{\text{RMS}}$ , but the voltage

decrease compared with the grid voltage is damped strongly. The sub-network load voltage RMS value does not drop below  $220 \text{ V}_{\text{RMS}}$ . The control algorithm tries to return the actual sub-network voltage to the set point. But within the voltage dip duration this could not be arranged. The injection of the reactive current in addition to the actual active current already fed in by the PV-invert can be seen clearly due to the phase difference between inverter current and load current during the voltage dip.

Analysing the effects of transient voltage variations in detail for several values of the decoupling inductor, minimal half cycle RMS values are measured during different types of voltage dips. Also different active power injections (25 kW, 50 kW and 75 kW) of Multi-PV and different load conditions (50 kW and 100 kW) for sensitive loads in the sub-network are considered. These are not marked differential in Figures 12 – 14, the differentiation results from the type of voltage dip. The reaction of phase 1 for a one phase voltage dip is shown in Figure 12, for a two phase voltage dip in Figure 13 and for a three phase voltage dip in Figure 14.

The conclusion of the diagrams is that using smaller values of the decoupling inductor result in deeper voltage dips for sensitive loads in the sub-network. Minimal voltage sag of  $205 \text{ V}_{\text{RMS}}$  for a decoupling inductor of 0.3 mH is measured. The differences between values of the decoupling inductor for 1.8 mH, 1.5 mH and 1.2 mH are slight,  $215 \text{ V}_{\text{RMS}}$  can be achieved for these inductors at minimum, which reduce the sag about 57 %.

Allowing a voltage deviation of  $\pm 10\%$  at most, a decoupling inductor of 0.6 mH is sufficient for considered voltage dips. If deeper voltage dips in the grid voltage occur and the operating mode is switched to ups service it has to be tested if for the chosen value of the inductor the desired classification according to EN 62040-3 can be achieved.

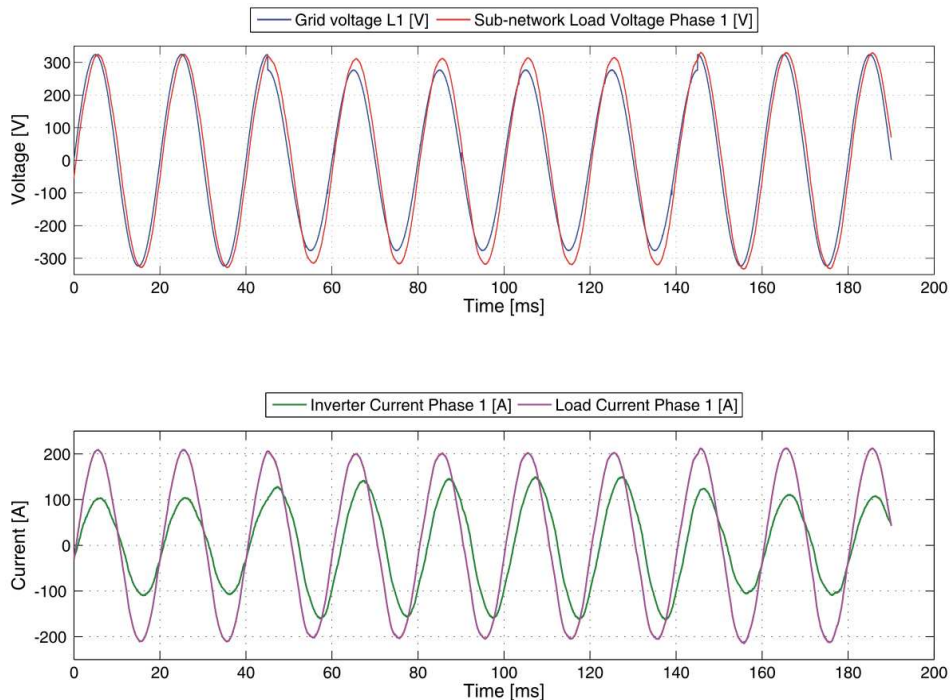


**Figure 11:** Transient voltages and current during a voltage dip. Parameters: 85 % remaining voltage, Duration time 100 ms, phase angle  $90^\circ$ ,  $P_{\text{MPV}} = 50 \text{ kW}$ ,  $P_{\text{sub-net}} = 100 \text{ kW}$ ,  $L_{\text{Dec}} = 0.6 \text{ mH} \dots 1.8 \text{ mH}$

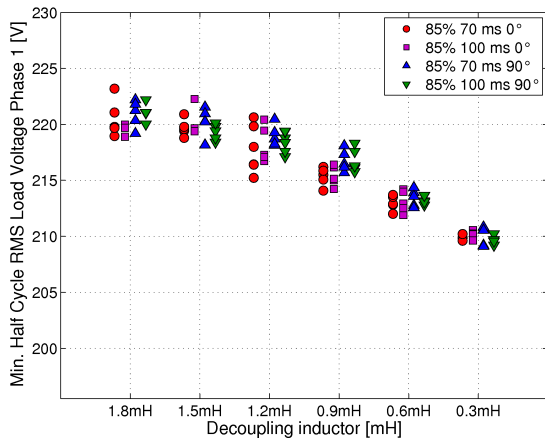


**Figure 12:** Reaction of load phase 1 at a one phase voltage dip with 85% remaining nominal voltage

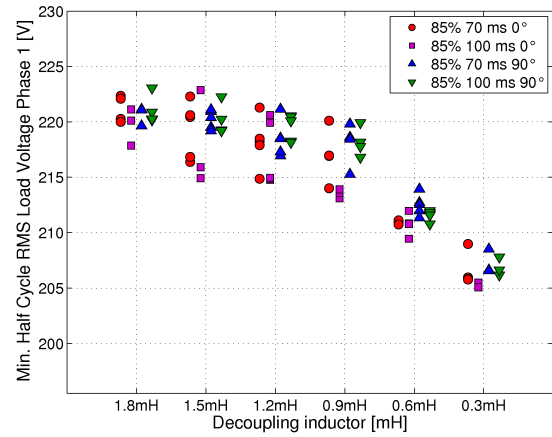


**Figure 14:** Reaction of load phase 1 at a three phase voltage dip with 85% remaining nominal voltage

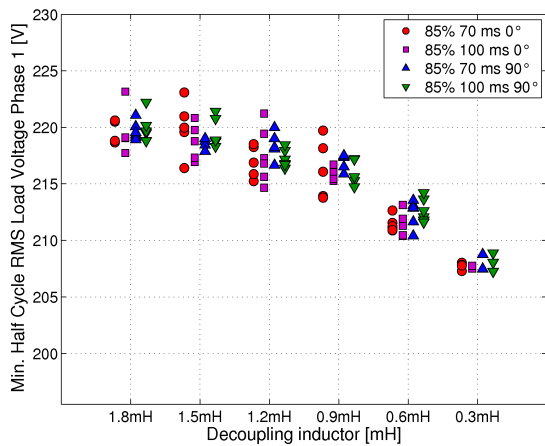


**Figure 13:** Reaction of load phase 1 at a two phase voltage dip with 85% remaining nominal voltage

For a better understanding of the measurement results shown in Figures 12-14, Table V quotes the average measured percentage reduction of grid voltage dips for sensitive loads in the sub-network split for several voltage dip conditions and decoupling inductors. For decoupling inductors with 1.8 mH the voltage dip can be reduced up to 73 %, decoupling inductors with 0.3 mH only achieve about 40 %.

#### 4.3. Voltage Quality Improvement

Powerful motors, fast changing loads or welding machines for example can cause high harmonic disturbances in industrial grids. If sensitive loads should work within this disturbed industrial grid, additional effort has to be undertaken to secure proper function of these loads.

The Multi-PV is able to provide for loads in the sub-network an improved voltage quality since inverters can produce a voltage profile with low harmonic content. A decoupling between the grid and the sub-network ensured by the decoupling inductor leads to a reduction of harmonics in the sub-network voltages. It is estimated that a stronger decoupling, achieved by a higher value of the inductor, will damp harmonics more effective.

In Figure 15 measurement results point out the prospects of different decoupling inductors for reduction of harmonics. Therefore the grid voltages are disturbed by several most typical odd harmonics in industrial grids ( $3^{\text{rd}}$ ,  $5^{\text{th}}$ ,  $7^{\text{th}}$ ,  $11^{\text{th}}$ ,  $13^{\text{th}}$  and  $17^{\text{th}}$ ). In total a THD-value of almost 9.5 % is achieved. According to the norm EN 61000 2-4 this industrial grid would range in class 3. With the smallest decoupling inductor (0.3 mH) a THD-value for sensitive loads in the sub-network of 7.11 % is possible; using 1.8 mH only 2.83% is feasible what results in an improvement into class 1 concerning the THD-value. All other tested inductor sizes lead to an enhancement from class 3 to class 2.

**Table V:** Average percentage reduction of grid voltage dip for sensitive loads in the sub-network

De-coupling inductor	3 phase voltage dip			2 phase voltage dip		1 phase voltage dip
	Phase 1	Phase 2	Phase 3	Phase 1	Phase 2	Phase 1
1.8 mH	73.00	76.14	76.23	70.27	76.94	72.76
1.5 mH	69.70	75.94	71.94	68.85	76.47	70.60
1.2 mH	66.04	66.72	70.43	63.79	71.35	66.12
0.9 mH	61.40	61.54	65.99	60.25	61.56	59.63
0.6 mH	46.49	46.77	48.09	47.79	50.16	51.30
0.3 mH	32.23	32.10	31.46	35.76	37.35	41.89

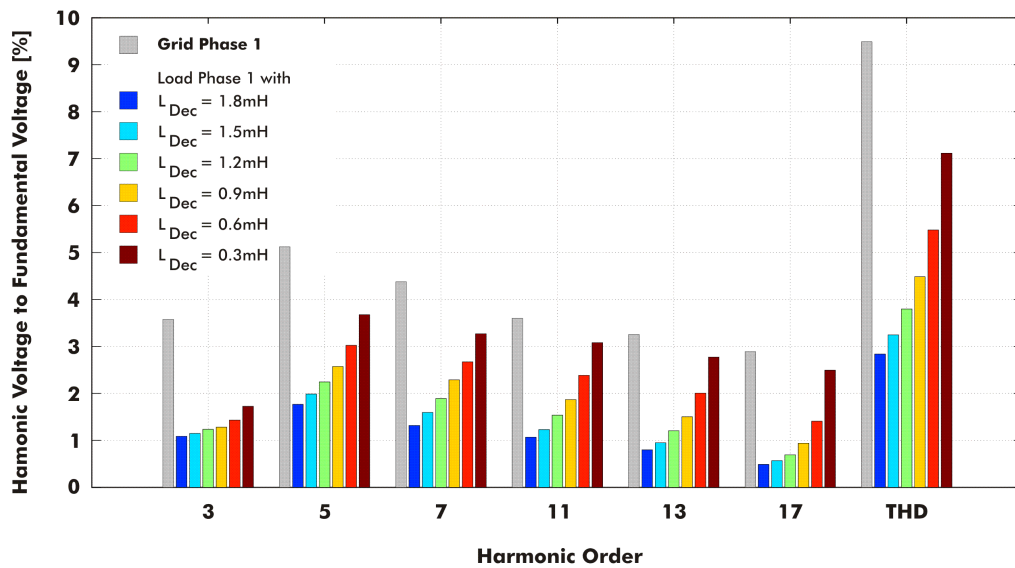


Figure 15: Harmonic reduction for various decoupling inductors for  $P_{MPV} = 50$  kW and  $P_{load} = 100$  kW

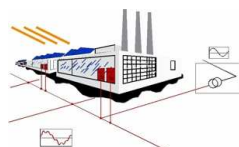
## 5 CONCLUSION

The measurements demonstrate that the Multi-PV System is able to compensate, reduce or damp grid voltage variations and harmonics for sensitive loads in the sub-network. Therefore the local Power Quality is improved. Furthermore the testing of several decoupling inductors shows the behaviour of different decoupling inductors. The optimal dimensioning of the decoupling inductor has to be made under consideration of following points and target aims

- Improvement of local voltage quality  
→ Higher value of the decoupling inductor
- Improvement of voltage support  
→ Higher value of the decoupling inductor
- Reduction of reactive power for the inverter  
→ Higher value of the decoupling inductor
- Reduction of ohmic losses  
→ Lower value of the decoupling inductor
- Cost effectiveness, weight, size  
→ Lower value of the decoupling inductor

## 6 ACKNOWLEDGEMENTS

The authors would like to thank the German Federal Ministry of Environment, Nature Conservation and Nuclear Safety for funding the project “Multi-PV Multifunktionale Photovoltaik Stromrichter – Optimierung von Industrienetzen und öffentlichen Netzen”(FKZ 0329943, see <http://www.multi-pv.de>).



Only the author is responsible for the content of this publication.

## 7 REFERENCES

- [1] M. Braun, T. Stetz: Multifunctional Photovoltaic Inverters – Economic Potential of Grid-Connected Multifunctional PV-Battery-Systems in Industrial Environment, 23<sup>rd</sup> European Photovoltaic Solar Energy Conference, Valencia, Spain, 1. - 4. September 2008
- [2] M. Braun, P. Strauss: A Review on Aggregation Approaches of Controllable Distributed Energy Units in Electrical Power Systems, International Journal of Distributed Energy Resources, Vol. 4, No. 4, pp 297-320, to be published in October 2008
- [3] A. Engler, J. Jahn: Inductive Decoupling of Low Voltage Sub-Networks, 9<sup>th</sup> International Conference on Electrical Power Quality and Utilization (EPQU), Barcelona, Spain, October 2007
- [4] J. Jahn: Energiekonditionierung in Niederspannungsnetzen unter besonderer Berücksichtigung der Integration verteilter Energieerzeuger in schwachen Netzausläufern, Universität Kassel, ISBN 978-3-89958-377-9
- [5] D. Geibel, J. Jahn, R. Juchem: Simulation model based control development for a multifunctional PV-inverter, 12th European Conference on Power Electronics and Applications, Aalborg, Denmark, September 2007
- [6] K. Heuck et al.: Elektrische Energieversorgung, 6. vollständig überarbeitete Auflage, Vieweg-Verlag, Wiesbaden